Title
Reoxidation of Chromium(III) Products Formed under Different Biogeochemical Regimes

Journal
Environmental Science and Technology, 51(9)

ISSN
0013-936X

Authors
Varadharajan, Charuleka
Beller, Harry R
Bill, Markus
et al.

Publication Date
2017-05-02

DOI
10.1021/acs.est.6b06044

Peer reviewed

Reoxidation of Chromium(III) Products Formed under Different Biogeochemical Regimes

Charuleka Varadharajan, Harry R. Beller, Markus Bill, Eoin L. Brodie, Mark E. Conrad, Ruyang Han†, Courtney Irwin‡, Joern T. Larsen§, Hsiao-Chien Lim∥, Sergi Molins, Carl I. Steefel, April van Hise⊥, Li Yang, and Peter S. Nico*

Earth and Environmental Sciences, Lawrence Berkeley National Laboratory, One Cyclotron Road, Berkeley, California 94720, United States

Environ. Sci. Technol., **2017**, *51* (9), pp 4918–4927

DOI: 10.1021/acs.est.6b06044

Publication Date (Web): April 3, 2017

*Phone: 510-486-7118; e-mail: psnico@lbl.gov.

Abstract

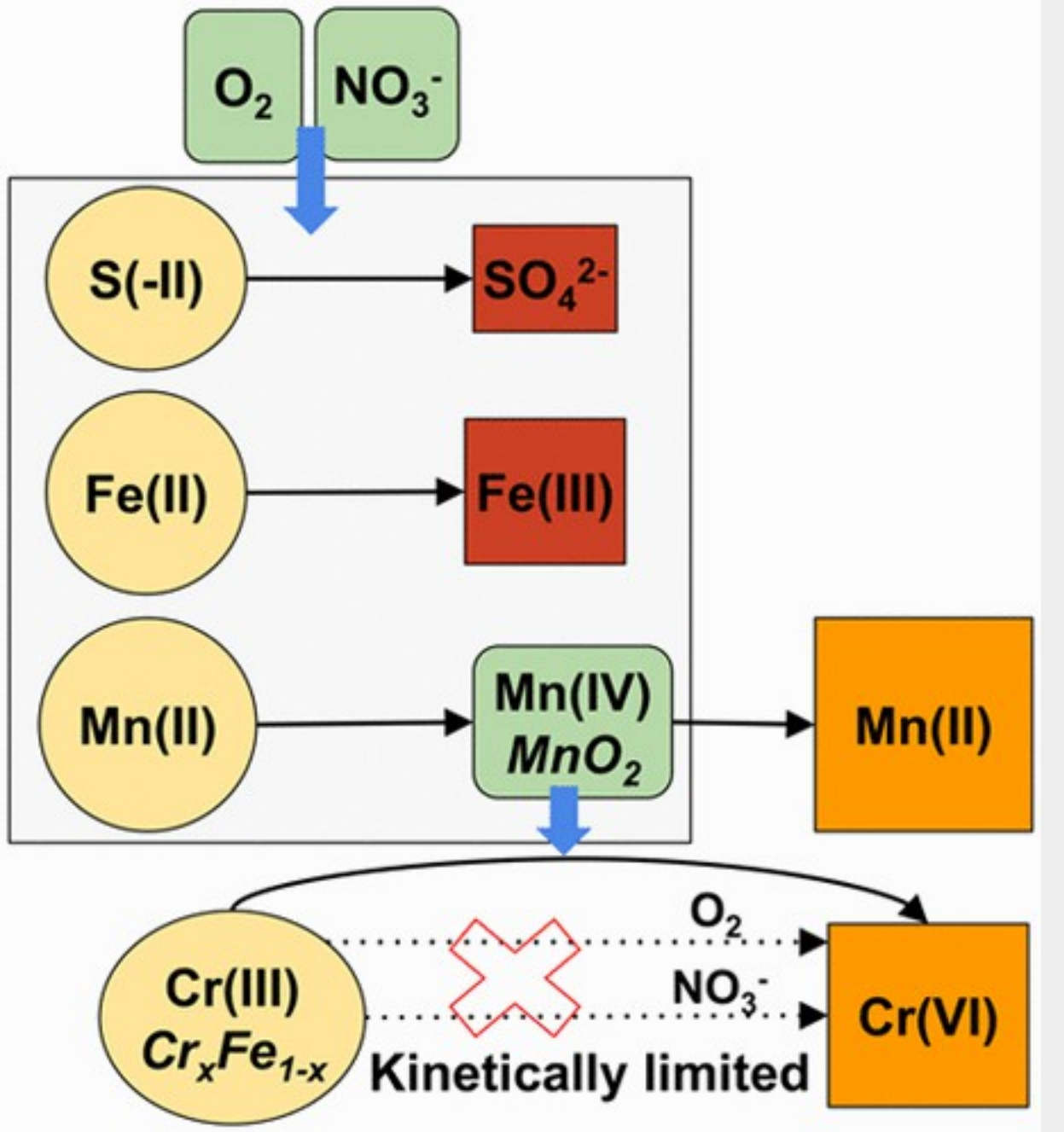

Hexavalent chromium, Cr(VI), is a widespread and toxic groundwater contaminant. Reductive immobilization to Cr(III) is a treatment option, but its success depends on the long-term potential for reduced chromium precipitates to remain immobilized under oxidizing conditions. In this unique long-term study, aquifer sediments subjected to reductive Cr(VI) immobilization under different biogeochemical regimes were tested for their susceptibility to reoxidation. After reductive treatment for 1 year, sediments were exposed to oxygenated conditions for another 2 years in flow-through, laboratory columns. Under oxidizing conditions, immobilized chromium reduced under predominantly

denitrifying conditions was mobilized at low concentrations (≪1 μM Cr(VI); ∼ 3% of Cr(III) deposited) that declined over time. A conceptual model of a limited pool of more soluble Cr(III), and a larger pool of relatively insoluble Cr(III), is proposed. In contrast, almost no chromium was mobilized from columns reduced under predominantly fermentative conditions, and where reducing conditions persisted for several months after introduction of oxidizing conditions, presumably due to the presence of a reservoir of reduced species generated during reductive treatment. The results from this 3-year study demonstrate that biogeochemical conditions present during reductive treatment, and the potential for buildup of reducing species, will impact the long-term sustainability of the remediation effort.

Introduction

Chromium is a common contaminant in groundwater and soils, since it is used in several industrial processes and can also be released from geologic sources.(1, 2) Chromium can exist in two stable oxidation states - the toxic and soluble hexavalent form, Cr(VI), and the relatively harmless and mostly immobile trivalent state, Cr(III). Reduction of Cr(VI) to Cr(III) for purposes of remediation can be achieved either by abiotic reaction of Cr(VI) with Fe(II), sulfide compounds, soil organic matter, or by microbially mediated direct or indirect reduction.(3-15) Treatment success is determined by the amount and rate of Cr(VI) reduction, as well as the stability of reduced products once the system returns to oxidizing conditions post-treatment.

Oxidation of Cr(III) by molecular oxygen, nitrate or other common oxidants is believed to be slow at moderate pH,(15, 16) despite Cr(VI) being thermodynamically stable in oxidized environments. This kinetic limitation on oxidation is crucial from a remediation perspective, because it means that it is feasible to maintain Cr in its reduced, insoluble state under transient or predominantly aerobic conditions, unlike other contaminants such as uranium, which are more readily reoxidized.(17, 18) Under moderate pH conditions, Mn(III/IV) (hydr)oxides, which are prevalent in the environment, appear to be the only potent naturally occurring oxidizers of Cr(III).(15, 16, 19, 20) Several factors control the potential for, rate and extent of Cr(III) reoxidation including the amount, mineralogy and surface properties of Mn oxides present, the structure and solubility of Cr(III) phases, and the degree to which dissolved Cr(III) can react with Mn oxide surfaces.(21) For example, chromium can be oxidized at different rates by a variety of Mn oxides including birnessite,(1, 22-27) δ-MnO_2,(19, 28) pyrolusite (β-MnO_2),(16, 25) todorkite,(24, 25) cryptomelane,(24) hausmannite(24, 29)and

hydrous manganese oxides.(30) Additionally, recent studies have shown that biogenic manganese oxides produced by bacterial oxidation of Mn(II) can result in freshly formed, amorphous phases that are more potent oxidizers of Cr(III) compared to aged or more crystalline phases.(31-33) Chromium(III) phases generally have low solubility. In particular, Cr(III) coprecipitated with Fe(III), a product of Cr(VI) reduction in natural environments, is significantly less soluble than pure Cr(III) phases.(34, 35) The presence of significant organic complexing agents, either microbial biomass/exudates or residual introduced organic matter, will increase the potential for Cr(III) reoxidation by forming soluble complexes with Cr(III).(36, 37) Chromium oxidation can be inhibited when reactive surfaces of manganese oxides are pacified due to precipitation of Cr(III) or other phases,(28, 37, 38) and competing influences by other ions including Mn(II) or Al(III).(23, 39)Finally, pH is a controlling variable, with solubility and oxidation rates generally decreasing at higher pH values.(16, 19, 23, 40)

When Mn(III/IV) oxides exist in the sediment, they are expected to be reduced and dissolved during the bioremediation process by direct microbial reduction or via reaction with microbially generated Fe(II) and sulfides. Thus, reoxidation of Cr(III) may be dependent on the reformation of Mn(III/IV) oxides from Mn(II). Although Mn(II) can be oxidized by O_2 and bacteria, significant Mn(II) oxidation is unlikely in an environment in which sulfide- and Fe(II)-containing compounds are maintaining reducing conditions. However, O_2 or nitrate can serve as electron acceptors for biotic and abiotic oxidation of sulfide- and Fe(II)-containing compounds. For this reason, introduction of substantial or continuing quantities of O_2 or nitrate into the reduced system could eventually deplete reserves of reduced Fe(II) and sulfide phases, creating conditions amenable to oxidation of Mn(II) to Mn(III/IV) oxides (Figure 1).

Figure 1. Pathways for Cr reoxidation following a reductive remediation treatment.

We investigated the potential for chromium immobilization under a variety of biologically stimulated conditions, and for remobilization of the reduced chromium following a return to oxidizing conditions, in a two-phase, 3-year experimental study using flow-through laboratory columns containing Hanford aquifer sediments (Figure 2). The study is unique due to the long-term observations of reduction and

reoxidation in flow-through columns using natural sediments, as compared to most previous studies (with one exception(41)) that were conducted over much shorter time scales (less than a month), with synthesized Cr(III) and Mn-oxides under controlled laboratory conditions.

Figure 2. Timeline of column operations throughout the study, and corresponding biogeochemical conditions in the columns.

The first phase of the experiment is presented in previous papers,(12, 42) where reducing conditions were maintained for ∼1 year in flow-through columns containing homogenized sediments from the Hanford 100H site. The columns were subject to lactate and Cr(VI) addition, and distinguished by different dominant electron acceptors present in Hanford groundwater [by addition of NO_3^- or SO_4^{2-}] or sediment [native Fe(III)]. As described previously, the columns evolved to have different biogeochemical conditions, mostly due to the different electron acceptors present in the influent solution.(42) Bulk chemical and microbial analyses suggested that denitrifying conditions were dominant in all nitrate-amended columns, and that conditions were less consistent across the sulfate-amended columns, with dominant fermentation and some sulfate reduction (evidenced by the presence of sulfide precipitates), present in some of the columns.(42) Chromate was depleted in all effluent solutions at varying quantities and rates, with the fastest and greatest amount of reduction occurring in the sulfate-amended columns with fermenting conditions.(42)

We also conducted extensive solid-phase characterization of the Cr(III) phases precipitated in the columns after the reductive treatments, the results of which are described in previous papers.(42, 43) In summary, the reduced Cr(III) phases were determined to be Cr–Fe hydroxides produced by the abiotic reaction of Cr(VI) with microbially reduced Fe(II). The products in all the columns were found to be structurally similar, despite the differences in the dominant biogeochemical reduction processes. It was hypothesized that local heterogeneity led to hotspots where reducing conditions differed from the dominant biogeochemical condition (such as detectable Fe reduction under predominantly denitrifying conditions, and sulfate reduction in predominantly fermenting environments), consequently leading to the formation of similar Cr–Fe precipitates under vastly different bulk biogeochemical conditions.(42, 43)

In this follow-on paper, we describe the second phase of the study, where the objectives were to (1) determine the potential for reoxidation of Cr(III) phases reduced in the various reductive

pretreatments, and (2) investigate the rates and potential mechanisms for Cr(III) reoxidation in the columns, if detected. In the reoxidation phase, the flow-though columns that had undergone different reductive pretreatments in Phase 1 were subjected to groundwater containing nitrate and oxygen for ~2 years, without addition of Cr(VI) or lactate. Effluent solutions were monitored over time to determine biogeochemical changes and the extent of Cr(III) reoxidation. At the end of the reoxidation phase, a series of pump manipulation tests was conducted to investigate the rates of and mechanisms involved in Cr(III) reoxidation.

Materials and Methods

Reduction Experiment and Solid-Phase Characterization of Reduced Cr(III) Phases

Experimental details of the reduction study are described elsewhere.(12, 42) Briefly, the reductive phase involved 11 columns (Figure 2) made using 6 mL, sterile, solid-phase extraction cartridges (7.8 cm (L) × 0.64 cm (i.d.)) packed with ~12 g of homogenized sediments from the Hanford 100H aquifer. The sand fraction of the Hanford formation sediment consists of quartz, plagioclase, hornblende, and mica (muscovite, biotite) with minor magnetite, orthoclase, and ilmenite, whereas the clay and silt fractions contain micas, vermiculite, chlorite (clinochlore), and ferruginous biedellite.(44) The columns were continuously exposed to anaerobic, synthetic groundwater containing Cr(VI), lactate, and different electron acceptors in a glovebox for 358 days (Table 1), and effluent solutions characterized as described below.

Table 1. Experimental Conditions for Reductive Treatment and Re-Oxidation (Also See Figure 2)

	reduction (358 days[a])	reoxidation (659 days[a])
atmospheric condition	anaerobic with an ultra–high purity N_2atmosphere maintained in a glovebox	Aerobic conditions maintained outside glovebox. Nitrogen gas was injected until day 42 into an inflatable glovebag to prevent oxidation of effluent samples prior to collection. A beaker containing NaOH pellets was used to scrub excess CO_2 in the glovebag for 66 days.

	reduction (358 days[a])	reoxidation (659 days[a])
influent solution (synthetic groundwater)	1.25 mM $NaHCO_3$, 1.6 mM $CaCl_2$, and 0.1 mM NH_4Cl, 1 mM K_3PO_4 buffer (pH 7), 5 uM Cr(VI)[a], 5 mM sodium lactate	1.25 mM $NaHCO_3$, 1.6 mM $CaCl_2$, 0.1 mM NH_4Cl, 1 mM K_3PO_4 buffer (pH 7), 2 mM NO_3^-.
	12 mM KNO_3 added to nitrate-amended columns	Sterilized using 0.2 µm PES filters.
	7.5 mM $MgSO_4$added to sulfate-amended columns	
flow conditions	3 µL/min in an upflow (bottom-up) mode using a multichannel syringe pump	3 µL/min in an upflow (bottom-up) mode using a multichannel peristaltic pump.

a

Three columns (N-D3, S-S/F, X-L1) were subject to reduction for an additional 449 days with 50 µM Cr (VI) in the stock solution. These columns were reoxidized for 210 days only.

Four columns (N-D4, S-F2, S-L2, and X-L2) were sacrificed for solid-phase and spectroscopic analysis at the end of the reduction experiment, as described previously.(42, 43) Selective extractions of the untreated and reduced column sediments were conducted by adding 10 mL of 0.5 N HCl to 0.5 g of air-dried sediment for 1 h,(45) and 24 h in a glovebox. Total Cr, Fe, and Mn concentrations in the extracts were determined using ICP-MS, and Fe(II) was measured using ferrozine.

Reoxidation Setup

The reoxidation phase was conducted using 7 columns representing the dominant biogeochemical characteristics prevalent in the reduction experiment (fermentation, denitrification, and low-lactate utilization/Cr reduction). The reoxidation phase began with 4 columns (N-D1, N-D2, S-F1, and S-L1) that had been reduced for 358 days. Three more columns (N-D3, S-S/F, X-L1) were added after being reduced for an additional 449 days under slightly altered conditions (Figure 2). Column N-D2 was taken down after 223 days of reoxidation.

All columns were initially flushed with chromate-free, deoxygenated influent solution to wash out residual Cr(VI) for ~22 h (2+ pore volumes) inside the glovebox prior to reoxidation. The columns were fitted with new autoclaved Tygon tubing attached with sterile 0.2 μm filters for delivery of injection and effluent solutions. The columns were then transferred outside the glovebox into aerobic conditions, and subject to influent containing oxygen and nitrate (naturally present in Hanford groundwater) as oxidants. Differences in the flow rates in each of the columns were minor (<0.5 mL/day).

After 659 days of reoxidation, a series of pump manipulation, stop-flow tests were conducted over ~3 months, where the pump was turned off for different periods of time (4, 7, 10, 14 days) and then restarted (SI Figure SI-1). In the final stage of the pump manipulation experiment (at 720 days), pyrophosphate, which is known to form strong complexes with Mn(III), was added to the influent solution to determine whether Mn(III) availability would impact the rate of Cr(III) oxidation.(46)

Effluent Solution Characterization

Effluent solutions in both phases of the study were collected in trace-metal clean centrifuge vials, and their solute composition was analyzed. Total element concentrations were determined by ICP-MS (PerkinElmer SCIEX ICP-Mass Spectrometer ELAN DRC II) after preserving samples with 2% (v/v) ultrahigh-purity nitric acid. Anion analyses included acetate, chloride, sulfate, nitrate, and phosphate by ion chromatography (Dionex model ICS-2100). Chromium speciation was determined for 21 samples collected over the duration of the reoxidation phase (SI Table SI-1) by passing effluent through IC-H cartridges and analyzing the resulting solution by ICP-MS. Samples were also collected for pH measurements and analyses of the concentration carbon isotope ratios of dissolved

inorganic carbon (DIC). Total DIC was measured in aliquots extracted with an airtight syringe and injected into helium-flushed 5.9 mL Labco exetainer vials containing 0.2 mL of 99.5% phosphoric acid (H_3PO_4). Concentrations and $\delta^{13}C$ of the resulting CO_2 were determined as in Torn et al.(47) All chemicals used in the experiments were reagent-grade or better and aqueous solutions were prepared with Milli-Q water (Millipore Elix 10 UV system).

Calculations

Solute concentrations represent net values after subtraction of respective blank sample concentrations. Concentrations of ions were calculated relative to the influent as in eq 1. Negative values represent depletion of the ion during reoxidation. $$C = C_{\text{effluent}} - C_{\text{influent}} \quad (1)$$, where C = ion concentration relative to the influent (μM), C_{effluent}=concentration in the effluent solution (μM), C_{influent}=concentration in the influent solution (μM) The amount of chromium deposited during reduction and mobilized during reoxidation in the columns was calculated from the sum of trapezoidal areas over consecutive measurements, in a plot of effluent concentration versus time (eq 2). Values below the detection limit (0.5 μg/L) were set to half the detection limit.(48)

$$Q \times 1440 \times 10^{-6} \times \sum_{n=2}^{n=\#\text{samples}} 0.5 \times (C_n - C_{n-1}) \times (t_n - t_{n-1}) \quad (2)$$

where Q = flow rate (3 μL/min), C_n = chromium concentration in sample n (μg/L), and t_n = time sample n was taken (days).

Results

Increase in Redox Potential Triggers Chromium Reoxidation in Nitrate-Amended Columns

Columns that were nitrate-amended and predominantly denitrifying prior to reoxidation (N-D1, N-D2, and N-D3) released small amounts of Cr in their effluent soon after their reducing capacities were exhausted and oxidizing conditions became prevalent, around days 50–66 (Figure 3a,d).

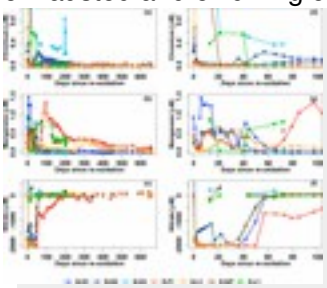

Figure 3. Chromium, manganese, and nitrate in the 7 columns for the entire period of the reoxidation experiment (left panel), and the first 100 days (right panel). The *x*-axis shows days adjusted to the start of the reoxidation phase in each of the columns. The *y*-axis has concentrations reported relative to influent values (eq 1). Negative nitrate values indicate consumption of influent nitrate during reoxidation. Note the

differences in the *y*-axis scale for each of the ions. (see SI Figure SI-2 for nitrite and sulfate. Concentration values are listed in SI Tables SI-3 to SI-7). Detection limits for chromium concentrations calculated relative to influent are ~0.01 μM.

In columns N-D1 and N-D2, denitrification and manganese reduction were prevalent prior to day 42 (under a nitrogen headspace) as indicated by the consumption of nitrate [effluent concentrations ~1–2 mM below influent] (Figure 3c,f), and the constant presence of nitrite [0.1–1 mM] (SI Figure SI-2a) and Mn [0.1–1.5 μM] (Figure 3b,e). During this period, corresponding Cr concentrations were low [~ 0.01–0.03 μM], after the first 3–5 days when some residual Cr(VI) from the reduction phase was still being washed out (Figures 3d and 4a). After the headspace was switched to ambient atmospheric conditions on day 42, nitrate depletion ceased with concentrations returning to influent levels [~ 2 mM] within 2 weeks, while nitrite and Mn concentrations dropped below the detection limit (Figure 4 and SI Figure SI-3). Small amounts of total chromium (0.02–0.24 μM) were released from both columns throughout the reoxidation phase, although concentrations declined over the first ~150–200 days, eventually reaching a steady rate of release. DIC concentrations in both columns were elevated for the first 42 days and then dropped back to influent levels after ~2 weeks (SI Figure SI-4). The $\delta^{13}C$ of the DIC was initially 5–10‰ lower than the influent, and returned to influent values after day 42. The elevated DIC concentrations and lower $\delta^{13}C$ values suggest that during the first ~42 days of reoxidation, there was continued metabolism of the low $\delta^{13}C$ lactate ($\delta^{13}C$ = –26‰) and/or metabolic byproducts of the lactate (e.g., biomass, biofilms) that was introduced into the columns during the pretreatment reduction phase. In either case, microbial activity appeared to cease after the first 6 weeks, coincident with changes in nitrate, nitrite, and Mn(II) concentrations, indicating a decrease of denitrifying activity in columns N-D1 and N-D2.

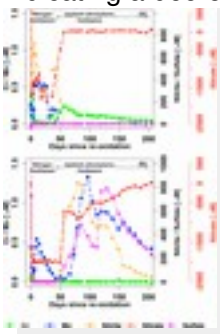

Figure 4. Comparison of conditions in (a) a representative denitrifying column N-D2, and in (b) fermenting column S-F1, during the initial period (200 days) after oxidative conditions were introduced. The *x*-axis shows days adjusted to the start of reoxidation in each of the columns. The *y*-axes have concentrations reported relative to influent values (eq 1). Negative nitrate values indicate consumption of influent nitrate

during reoxidation. The dashed line is drawn at day 42, when conditions where switched from a nitrogen headspace to ambient atmospheric conditions.

In contrast, column N-D3, which had an additional 449 days of reductive pretreatment, was introduced to ambient atmospheric conditions from the start of its reoxidation phase. Effluent nitrate concentrations were at influent levels [2 mM] as soon as reoxidation commenced (Figure 3c), and concentrations of nitrite were always low [0–10 μM], except on day 13 (~100 μM) (SI Figure SI-2a). Chromium released from N-D3 (0.2–2.35 μM) was at times almost an order of magnitude higher than the Cr released from N-D1 and N-D2, and continued to remain elevated after 210 days of reoxidation (Figure 3a).

Speciation tests using IC-H cartridges showed that Cr present in the effluent of all the nitrate-amended columns was mostly >90% Cr(VI) (SI Table SI-1). However, the cumulative Cr released at the end of the full reoxidation period (>600 days) represented a small fraction (<3%) of the total amount of Cr deposited during the reductive pretreatment (Table 2). The pH in all columns generally followed the same trends, and ranged from ~7.5 to 9.5 throughout the experiment (SI Figure SI-5).

Table 2. Amount of Chromium Deposited during Reduction and Mobilized during Re-Oxidation (Prior to the Pump Manipulation Tests) In the Columns Calculated as in eq 2[a]

column symbol	estimated total Cr deposited after reductive treatment [ug]	estimated total Cr release during reoxidation [ug]	% Cr released during reoxidation
N-D1	260	3.3	1.3%
N-D2	260	4.4	1.7%
N-D3	900[b]	18	2.8%
S-F1	370	1.1	0.3%

column symbol	estimated total Cr deposited after reductive treatment [ug]	estimated total Cr release during reoxidation [ug]	% Cr released during reoxidation
S-S/F	2400[b]	1.3	0.0005%
S-L1	180	1.5	0.4%
X-L1	760[b]	3.9	0.8%

a

Values were rounded to two significant digits. Some carryover of solutions from the reduction phase was observed in the first week of the re-oxidation phase, but did not significantly impact the percent of total Cr released during re-oxidation.

b

This is an approximate estimate of the total Cr deposited in the column. Sampling stopped during the reduction phase (day 608 for column N-D3 and day 585 for columns S-S/F and X-L1), which lasted for a total of 807 days for these 3 columns. Chromium consumption stabilized in N-D3 and X-L1 after 390 days of reduction; thus the average Cr concentration from day 390 onward was used to estimate the amount of Cr deposited for the period where data were unavailable. Conditions were more dynamic in S-S/F, and the average concentration from days 553 onward were extrapolated to the end of reduction.

Insignificant Chromium Reoxidation in Other Columns

In column S-F1, where fermentative conditions were dominant during the reductive pretreatment, nitrate and manganese reducing conditions persisted through the reoxidation phase, indicated by consumption of nitrate and presence of effluent nitrite [up to ~1 mM above influent] for ~1 year (Figure 3c and SI Figure SI-2a), and elevated Mn [0.1–1.33 μM above influent] for the entire >600 days (Figure 3b). No detectable Cr was released from S-F1 after the first ~3 day washout period

(Figures 3a and 4b). Sulfate was also measured in the effluent [0–0.8 mM] during the first ~300 days of reoxidation, suggesting the occurrence of sulfide oxidation (SI Figure SI-2b).

In column S-S/F, which had been reduced for an additional 449 days, no effluent Cr was detected after the initial washout period, (Figure 3a). Effluent Mn was observed consistently [0.03–0.6 μM], peaking between days 250–400 (Figure 3b).

For S-L1, which had low levels of lactate consumption and reducing activity during the reductive pretreatment, Cr was nondetectable in the effluent after the initial washout period (Figures 3a). In X-L1, for which the dominant available electron acceptor during the reductive pretreatment was native Fe(III), some Cr [0.3–0.6 μM] was released in the first 40 days after reoxidation (Figure 3d). However, the total Cr released during reoxidation amounted to ~0.8% of the total Cr that had been deposited during the reductive phase. Corresponding Mn concentrations were low during this period and increased after day 40, after which chromium dropped to nondetect values, indicating that reducing activity may have rebounded in the column after day 40.

Pump Manipulation Experiment Results

Elevated total chromium concentrations, relative to steady-state, were measured following stop-flow events in N-D1 (0.01–0.1 μM), and by an order of magnitude more in N-D3 (0.2–2 μM) (Figure 5a, SI Figure SI-6); column N-D2 had been taken down on day 223, and was not subject to the stop-flow tests. The extent of increase was linearly proportional to the pump-stoppage period (Figure 5a). Chromium levels did not increase after stop-flow events in any other column. The addition of pyrophosphate did not substantially affect Cr concentrations, except perhaps for a small decrease in N-D3 concentrations (SI Figure SI-6).

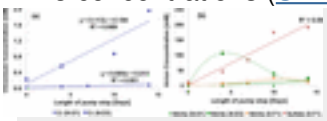

Figure 5. Results from the pump manipulation experiment. Comparison of (a) chromium, (b) nitrite and sulfate concentrations (relative to influent) from three columns N-D1, N-D3, and S-F1 with corresponding pump stop length. The slopes of the trendlines in (a) represent Cr oxidation rates in columns N-D1 and N-D3. Concentrations on the last day prior to the start of the pump manipulation were used to represent “zero” days of pump stoppage.

In N-D3, the greatest detectable nitrite concentrations were observed after a 4-day stop-flow event (Figure 5b). The decrease in detectable nitrite with longer stoppage times is consistent with its role as a reactive intermediate in the nitrate reduction pathway. Elevated nitrite concentrations were observed to a smaller extent in N-D1 and S-F1. Sulfate concentrations were elevated in S-F1, proportional to stop-flow event length (Figure 5b).

Selective Extractions of Reduced Column Sediments

All the different pretreatments had lower extractable Mn, relative to original Hanford sediment (Figure 6a, SI Table SI-2). However, the loss was greatest in S-F2 (~25–35%), about half of which was lost from the bottom section. Columns N-D4 and S-S/F had similar amounts of Mn loss (~15%).

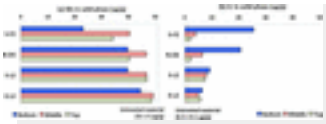

Figure 6. Acid-extractable manganese and chromium concentrations (μg/g) from the 1 h 0.5 N HCl extractions in column sediments sacrificed after the reduction phase compared to reference material from Hanford (see SI Table SI-2).

Extractable Cr (Figure 6a) and Fe measurements from the reduced column sediments (SI Table SI-2) showed that the maximum amount of chromium deposition occurred in columns S-F2 and N-D4, near their inlets (bottom sections),(42, 43) and were ~100 times the background level (of untreated Hanford sediment). Column S-F2 had the greatest amount of acid-extractable Fe(II) values, exceeding the background level by a factor of 2 near the column inlet. The other three columns had extractable Fe(II) concentrations exceeding background levels by 10 to 20%.

Discussion

Sources and Rates for Chromium Remobilization under Oxidizing Conditions in Nitrate-amended and Unamended Columns

The results indicate that chromium was mobilized in the nitrate-amended columns when the redox potential increased, and notably during periods when effluent Mn concentrations were low (indicating lower Mn reduction activity) (SI Figure SI-7). In columns N-D1 and N-D2, Mn concentrations dropped quickly prior to a pulse of Cr release (Figure 4a and SI Figure SI-3a), suggesting a possible role for freshly formed manganese oxides, which can be more reactive than aged, crystalline phases,(31, 32) in Cr reoxidation.

The observations can be explained by a conceptual model, with two source terms: (1) a limited pool of more soluble Cr(III) that was quickly reoxidized and released in a pulsed manner and (2) a larger, relatively insoluble pool that was steadily reoxidized at a slower rate. This conceptual model is consistent with recent work showing that Cr(VI) production in diffusion limited systems such as structured soils/sediments is highly dependent on the solubility of the Cr(III) phases, where the rate limiting steps are the dissolution of Cr(III) solids and the diffusive transport to Mn oxides.(49) An additional possibility for the fast pulsed release is the reaction of soluble Cr(III) with Mn oxides

located near the Cr(III) phases, at small separation distances, thereby minimizing diffusive transport times. Over time, the closer Mn oxides get consumed, leading to an increase in separation distances (and hence transport times) to other Mn oxides.(49)

Sources of the rapidly mobilized, soluble Cr pool in the nitrate-amended columns could be organically complexed Cr(III) (either the product of enzymatic Cr(VI) reduction or Cr(III) concentrated in organic/cellular matter), Cr(III) sorbed on mineral surfaces, or poorly crystalline Cr(III) phases.(42, 43) Although, previous spectroscopic analysis confirmed that the major Cr reduction products in all the columns were Cr(III)–Fe(III) mineral phases, minor phases could still be present.(42, 43)

In contrast, the source of the slow-release Cr pool could be dissolution and subsequent oxidation of Cr(III)–Fe(III) hydroxides precipitated during the reduction pretreatment. Although the solubility of Cr–Fe hydroxide (abiotic or microbially mediated) reduction products at pH 7 to 10 has not been directly measured since they are relatively insoluble at pH values above 6, one can infer that solubilized aqueous Cr concentrations would be on the order of 10^{-7} to 10^{-8} M (assuming the composition of Cr–Fe precipitates in this study is $Cr_{0.25}Fe_{0.75}(OH)_3$(43)), based on $Cr(OH)_3$solubility at pH 4 to 14,(35) and Cr–Fe hydroxide solubility at pH 2 to 6.(34) For comparison, the steady state chromium concentration measured in column N-D1 was ~3×10^{-8} M.

Based on the theory that solubility is the rate-limiting step, release rates for the two hypothetical pools can be inferred from the pump manipulation experiments, where longer equilibration times would lead to increased dissolved Cr concentrations. The slopes of the trendlines obtained from plotting chromium concentrations in columns N-D1 and N-D3 against stop-flow event length were used to obtain first-order release rates (Figure 5a). Column N-D3, which was only oxidized for 210 days, had continual, pulsed releases of Cr, indicating the possible presence of the more soluble Cr(III) pool. A fast release rate of 0.1 μM.d^{-1} (~0.006 μM·d^{-1}·$\mu mol^{-1}_{Cr\ deposited}$, when normalized by Cr deposited in the column during reduction] was calculated using Cr concentrations in N-D3 following stop-flow events (0.2–2 μM)] (Figure 5a). In contrast, column N-D1, which was oxidized for 659 days, had reached a steady state of release (Figure 3), presumably from a slow-release pool. A slow-release rate of 0.005 μM·d^{-1} (~0.001 μM·d^{-1}·$\mu mol^{-1}_{Cr\ deposited}$) was calculated from Cr concentrations in N-D1 following stop-flow events (0.01–0.1 μM), which is lower than in N-D3 by a factor of 20 (or a factor of 6, when normalized by Cr deposited) (Figure 5a). For comparison, the slow-release rate calculated using the stop-flow experiment is similar to an alternate slow-release rate calculation of 0.002–0.005 μM·d^{-1} in N-D1 and N-D2, obtained by assuming uniform chromium release rates for all samples collected from day 170 onward (as eq 2 divided by remaining days of reoxidation).

Other studies that have measured chromium oxidation rates at neutral pH have reported a variety of rates (Table 3). It is difficult to make a direct comparison of rates given differences in experimental conditions, especially considering that the other studies were conducted over much shorter time scales (none longer than a month), under idealized laboratory conditions, using various concentrations of synthesized Cr(III) and Mn-oxides. Despite the differences in the experimental settings, the rates calculated here are comparable with previously reported oxidation rates. Notably, several studies observed higher initial rates that declined over time as the system approached steady state.

Table 3. Comparison of Published Cr(III) Oxidation Rates, With Measurements Conducted at Neutral pH (7-8) for at Least 1 Week

reference	Cr(III) species	Cr(III) reoxidation rates	experimental conditions
Eary and Rai (1987)(16)	$Cr(OH)_3$	slow rate (estimated from concentrations of Cr(VI) released in 150–600 h): ~0.03 $\mu M \cdot d^{-1}$	9.6×10^{-5} M Cr(III)(s) with A/V= 35.6 $m^2.L^{-1}$ reacted with MnO_2 at pH 8.3 for 25 days
Oze et al. (2007)(1)	chromite $[FeCr(III)_2O_4]$	0.001 $\mu M.d^{-1}$ at pH 7, dropping to zero at pH 8	0.3 g Cr(III) reacted with 0.86 g birnessite at pH 3–8 for 19 days
		estimated from equation: $d[Cr(VI)]/dt = 0.26\ pH^2 – 4.1\ pH + 16$	

reference	Cr(III) species	Cr(III) reoxidation rates	experimental conditions
Rajapaksha et al. (2013)(27)	chromium(III)-muscovite [Fuschite]	slow rate: 0.03 μM·d^{-1} fast rate (first 25 h): 0.1 μM·d^{-1}	8 g/L Cr(III) reacted with 4 g/L birnessite at pH 8 (study was conducted at pH 5–8) for ∼10 days
Namgung et al. (2014)(29)	$Cr(OH)_3$	zero at pH 7, 0.08–0.1 μM·d^{-1} at pH 8.	1.0 g/L Cr(III) reacted with 50 μM Mn(II) at pH 7–9 under oxic conditions for 25 days
Tang et al. (2014)(32)	$CrCl_3$	initial rates (first 20 h): 2–8 μM·d^{-1} under light conditions. 0.5–2 μM·d^{-1}under dark conditions. approximate calculated steady state rate (at 200 days), assuming a linear increase in concentrations over time: 0.2–1 μM.d^{-}	50 μM Cr(III) reacted with ∼40 μM biogenic manganese oxides resuspended in an organic carbon-rich medium (K medium) at pH 6.2/7.2 under light and dark conditions for 8.3 days

reference	Cr(III) species	Cr(III) reoxidation rates	experimental conditions
		[1]under light conditions. 0.2–0.5 μM.d^{-1} under dark conditions.	
		rates varied with age of manganese oxides.	
Butler et al. (2015)(22)	Cr(III) precipitate from abiotic reaction of FeS with Cr(VI)	average rate: 0.07 μM·d^{-1} [1]with higher initial rates slowing over time.	31 mg/L Cr(III) reacted with 165 mg/L birnessite at pH 7.5 for 20 days
Hausladen and Fendorf (2017)(49)	Cr $(OH)_3$, $Cr_{0.25}Fe_{0.75}(OH)_3$	initial rates (first 2 days): 2 μM·d^{-1}, decreasing after ∼10 days to <0.1 μM·d^{-1}	Cr(III)-coated quartz grains in flow-through columns, reacting with 0.23 mM Mn(II) at pH 7.6 for 50 days

reference	Cr(III) species	Cr(III) reoxidation rates	experimental conditions
this study	Cr–Fe hydroxides	slow rate: 0.005 μM·d^{-1}	2-year flow-through columns at pH 7–9, initially subject to reductive treatment for 1 year
		fast rate: 0.1 μM·d^{-1}	

Another possible reason for the Cr release observed in the unameded column X-L1 is desorption of Cr(VI) that was not fully reduced. Spectroscopic analysis of column X-L2 showed that there could be ∼10% Cr(VI) remaining in the solid phase of unamended columns after reduction.(43)Cr(VI) desorption was also found to occur in another study where Cr(III) (reduced by a mixture containing *Desulfovibrio vulgaris* strain RCH1 and hematite/Al-goethite) was reacted with birnessite over 10–50 days.(22)

Environmental Implications for the Stability of Cr(III) Products Reduced under Different Biogeochemical Conditions

The results indicate that Cr(III) reduced under sulfate-reducing or fermenting conditions is more likely to remain immobilized for a longer period, compared to Cr(III) produced under denitrifying conditions. There are several possible explanations for the results:

1. *Buffering of Reductive Redox Status*. Solid-phase reduced species (e.g., Fe(II) phases, sulfides, microbial bio(necro)mass) accumulated during the reduction pretreatment,(42) can lead to persistence of reduced conditions, well beyond the duration of treatment. Reduced species can scavenge oxidants of Mn(II) and Cr(III), and potentially rereduce any Mn or Cr that may have been oxidized. Other studies have also found anoxia or reduced species such as FeS to have an inhibitory effect on chromium oxidation by manganese oxides.(29, 50)

2. *Extent of Solid-Phase Manganese*. Strongly reducing conditions can lead to a substantial loss of solid-phase manganese, including manganese oxides, which are the only potent oxidizers of Cr at higher pH. This was evident in S-F2, which lost a substantial amount of solid-phase Mn (∼25–30%), about half of which was from

the bottom section (Figure 6a). About 80% of the Cr(III) deposition in S-F2 was also concentrated in the bottom section, where the extracted Cr:Mn ratio was ∼1:1 (Figure6b). For comparison, the Cr:Mn ratio in the bottom section of N-D4 was ∼0.5. Given that some additional loss of Mn from column S-F1 also occurred during the reoxidation phase, the opportunity for precipitated Cr(III) to be reoxidized in fermenting columns could be substantially decreased due to loss of solid-phase Mn from the same location. However, this possibility may not apply for a natural system where groundwater recharge of dissolved Mn could occur.

3. *Inaccessibility of Oxidative Surfaces*. Strongly reducing conditions can lead to inhibition of Cr(III) oxidation due to the potential competing influence of Mn(II) on manganese oxide surfaces,(23) or surface precipitation on manganese oxide surfaces by reduced species such as sulfides or Cr-(oxy)hydroxides.(28, 37)

4. *Lack of Higher Solubility Cr(III)* phases- Enzymatic reduction of Cr(VI) resulting in soluble organic Cr(III) products may have occurred to a greater extent in the nitrate-amended columns. Although the reduced Cr phases in all the columns were identified to be predominantly Cr–Fe precipitates, extensive Fe(III) reduction under denitrifying conditions is thermodynamically unfavorable, and thus denitrifying columns have the greatest likelihood to contain other soluble organically complexed Cr(III) species. For example, in another study, Cr(VI) reduced in the presence of*Desulfovibrio vulgaris* strain RCH1 and hematite/Al-goethite, was concentrated as Cr–Fe hydroxide nanoparticles in biofilms. (22) However, extensive Fe(III) reduction was observed in the sulfate-amended fermenting columns, favoring the formation of relatively insoluble Cr–Fe coprecipitates, since the rates of Cr(VI) reduction by Fe(II) are much greater than those for enzymatic reduction. Thus, strongly reducing conditions that promote Fe(III) reduction will also decrease the potential for enzymatic reduction of Cr, and limit the production of the more soluble organically complexed Cr (III) pool.

The data from this study suggest a dominant role for the first and fourth possibilities as evidenced by the long-term sulfate and Mn reduction in columns S-F1 and S-S/F and the higher rate of Cr reoxidation in N-D3 compared to N-D1, even after accounting for excess Cr reduced over the

additional 449 days of reductive pretreatment (rates for N-D3 were a factor of 6 more than N-D1, when normalized by the amount of Cr deposited in the columns during reduction).

Thus, biogeochemical conditions during reductive treatments of Cr(VI) can impact the long-term stability of the remediation effort. If treatment is conducted using nitrate reducing conditions, slow, sustained reoxidation of Cr(III) (at a rate on the order of 0.005 $\mu M.d^{-1}$) can occur when the system is returned to oxidizing conditions, leading to release of Cr(VI) at low concentrations for many years, depending on the mass of Cr precipitated. While slow reoxidation is unlikely to impact groundwater with higher flow-rates, such as Hanford (flow rates ∼1–15 m/d(51)), it can potentially have a detrimental impact on remediation in other groundwater systems with slow flow rates (on the order of 1 m per decade), depending on oxidant availability.

The results imply that addition of sulfate as an electron acceptor to organically stimulated bioremediation treatments, in order to foster accumulation of reduced species by attaining sulfate-reducing or fermentative conditions, might be beneficial in ensuring the long-term immobilization of reduced Cr(III) products. This may be particularly important in heavily Cr-contaminated sites, where the long-term stability of Cr(III) is dependent on Mn redox status, and where it has been shown that organic carbon or other reducing agents added to stabilize Cr(III) also need to reduce Mn(III/IV) species.(41)

Supporting Information

The Supporting Information is available free of charge on the ACS Publications website at DOI: 10.1021/acs.est.6b06044.

- Pump manipulation experiment timeline, effluent data during reoxidation for flow-through columns (PDF)

- **PDF**
  - es6b06044_si_001.pdf (1.71 MB)

Reoxidation of Chromium(III) Products Formed under Different Biogeochemical Regimes

S
1

Re-oxidation of chromium(III) products formed under different biogeochemical regimes: Supporting

Information

Charuleka Varadharajan
[†]
, Harry R. Beller
[†]
, Markus Bill
[†]
, Eoin L. Brodie
[†]
, Mark E. Conrad
[†]
, Ruyang
Han
[†‡]
, Courtney Irwin
[†§]
, Joern T. Larsen
[†&]
, Hsiao-Chien Lim
[†#]
, Sergi Molins
[†]
, Carl I. Steefel
[†]
, April Van
Hise
[†^]
, Li Yang
[†]
, and Peter S. Nico
[†*]
[†]
Earth and Environmental Sciences, Lawrence Berkeley
National Laboratory, One Cyclotron Road,
Berkeley, California, 94720
CORRESPONDING AUTHOR
*Peter S. Nico (
psnico@lbl.gov
), Lawrence Berkeley National Laboratory, One Cyclo
tron Road,
Berkeley California, 94720. Ph: 510-486-7118.
Number of pages: 20 (including cover)
Number of figures: 7
Number of tables: 7
PRESENT ADDRESS:
[‡]
Assembly Biosciences, 12085 Research Drive, Alachu
a, FL 32615
[§]
Brelje and Race Labs, 425 S. E St. Santa Rosa, CA
95404
[&]
Apple Inc., Environmental Technologies Group, 1 In
finite Loop, Cupertino, CA 95014
[#]
Color Genomics, 1801 Murchison Drive #128, Burling
ame, CA 94010
[^]
Mechanical and Aerospace Engineering, University o
f California, Davis, CA 95616
S
2
Supplementary Information Figures
Figure SI-1
Timeline of pump-manipulation experiments.
Figure SI-2
Nitrite and sulfate in the 7 columns for the entir
e period of the re-oxidation experiment (left
panel), and the first 100 days (right panel). The x
-axis shows days adjusted to the start of the re-ox
idation
phase in each of the columns. The y-axis has concen
trations reported relative to influent values (Equa

tion
1). Note the differences in the y-axis scale for ea
ch of the ions. Concentration values are listed in
Tables
SI-3 to SI-7).
Figure SI-3
Comparison of conditions in (a) denitrifying column
N-D1, and in (b) and in the sulfate-
amended low activity column S-L1, during the initia
l period (200 days) after oxidative conditions were
introduced. The x-axis shows days adjusted to the s
tart of re-oxidation in each of the columns. The y-
axes
have concentrations reported relative to influent v
alues (Equation 1). Negative nitrate values indicat
e
consumption of influent nitrate during re-oxidation
. The dashed line is drawn at day 42, when conditio
ns
where switched from a nitrogen headspace to ambient
atmospheric conditions.
Figure SI-4
DIC, nitrate concentrations (relative to influent
as in Equation 1) and
δ
13C of the DIC for
250 days after oxidative conditions were introduced
. The nitrate-amended columns are shown in the left
panel, and the sulfate-amended columns are shown in
the right panel. The dashed line indicates day 42.
Figure SI-5
pH values in the 7 columns and influent solution fo
r the entire period of the re-oxidation
experiment. The x-axis shows days adjusted to the s
tart of the re-oxidation phase of the experiment. p
H
values for the first 66 days were slightly higher d
ue to NaOH pellets that were used to scrub CO_2
from the
glove bag.
Figure SI-6
Influent-subtracted concentrations of various ions
in the column effluents during the pump
manipulation experiments (calculated as $C=C_{effluent}-C_{influent}$
). The x-axis shows days adjusted to the start of
the pump manipulation. Note the differences in the
y-axis scale for each of the ions.
Figure SI-7
Effluent chromium and manganese concentrations in
the denitrifying columns.

†Author Present Address

(R.H.) Assembly Biosciences, 12085 Research Drive, Alachua, Florida 32615, United States.

‡Author Present Address

(C.I.) Brelje and Race Laboratories, 425 S. E St. Santa Rosa, California 95404, United States.

§Author Present Address
(J.T.L.) Apple Inc., Environmental Technologies Group, 1 Infinite Loop, Cupertino, California 95014, United States.

‖Author Present Address
(H.-C.L.) Color Genomics, 1801 Murchison Drive #128, Burlingame, California 94010, United States.

⊥Author Present Address
(A.v.H.) Mechanical and Aerospace Engineering, University of California, Davis, California 95616, United States.

The authors declare no competing financial interest.

Acknowledgment

This work was supported as part of the Berkeley Lab Sustainable Systems Scientific Focus Area funded by the U.S. Department of Energy, Office of Science, Office of Biological and Environmental Resources, Subsurface Biogeochemical Research program under contract number DE-AC02-05CH11231. The Advanced Light Source (ALS) is supported by the Director, Office of Science, Office of Basic Energy Sciences, of the U.S. Department of Energy under Contract No. DE-AC02-05CH11231.

Reference QuickView

References

This article references 51 other publications.

1. 1.

Oze, C.; Bird, D. K.; Fendorf, S. Genesis of hexavalent chromium from natural sources in soil and groundwater *Proc. Natl. Acad. Sci. U. S. A.* **2007**, 104 (16) 6544– 6549 DOI: 10.1073/pnas.0701085104

[Crossref], [PubMed], [CAS]

2. 2.

Izbicki, J. A.; Wright, M. T.; Seymour, W. A.; McCleskey, R. B.; Fram, M. S.; Belitz, K.; Esser, B. K. Cr(VI) occurrence and geochemistry in water from public-supply wells in California *Appl. Geochem.* **2015**, 63, 203–217 DOI: 10.1016/j.apgeochem.2015.08.007

[Crossref], [CAS]

3. 3.

Manning, B. A.; Kiser, J. R.; Kwon, H.; Kanel, S. R. Spectroscopic Investigation of Cr(III)- and Cr(VI)-Treated Nanoscale Zerovalent Iron *Environ. Sci. Technol.* **2006**, 41 (2) 586– 592 DOI: 10.1021/es061721m

[ACS Full Text]

4. 4.

Fendorf, S.; Wielinga, B. W.; Hansel, C. M. Chromium Transformations in Natural Environments: The Role of Biological and Abiological Processes in Chromium(VI) Reduction *Int. Geol. Rev.* **2000**, 42 (8) 691– 701DOI: 10.1080/00206810009465107

[Crossref]

5. 5.

Sedlak, D. L.; Chan, P. G. Reduction of hexavalent chromium by ferrous iron *Geochim. Cosmochim. Acta***1997**, 61 (11) 2185– 2192 DOI: 10.1016/S0016-7037(97)00077-X

[Crossref], [CAS]

6. 6.

Buerge, I. J.; Hug, S. J. Kinetics and pH Dependence of Chromium(VI) Reduction by Iron(II) *Environ. Sci. Technol.* **1997**, 31 (5) 1426– 1432 DOI: 10.1021/es960672i

[ACS Full Text], [CAS]

7. 7.

Eary, L. E.; Rai, D. Chromate removal from aqueous wastes by reduction with ferrous ion *Environ. Sci. Technol.* **1988**, 22 (8) 972– 977 DOI: 10.1021/es00173a018

[ACS Full Text], [CAS]

8. 8.

Wielinga, B.; Mizuba, M. M.; Hansel, C. M.; Fendorf, S. Iron Promoted Reduction of Chromate by Dissimilatory Iron-Reducing Bacteria *Environ. Sci. Technol.* **2000**, 35 (3) 522– 527 DOI: 10.1021/es001457b

[ACS Full Text]

9. 9.

Hansel, C. M.; Wielinga, B. W.; Fendorf, S. Structural and compositional evolution of Cr/Fe solids after indirect chromate reduction by dissimilatory iron-reducing bacteria *Geochim. Cosmochim. Acta* **2003**, 67 (3)401– 412 DOI: 10.1016/S0016-7037(02)01081-5

[Crossref], [CAS]

10. 10.

Patterson, R. R.; Fendorf, S.; Fendorf, M. Reduction of Hexavalent Chromium by Amorphous Iron Sulfide*Environ. Sci. Technol.* **1997**, 31 (7) 2039– 2044 DOI: 10.1021/es960836v

[ACS Full Text], [CAS]

11. 11.

Narayani, M.; Shetty, K. V. Chromium-Resistant Bacteria and Their Environmental Condition for Hexavalent Chromium Removal: A Review *Crit. Rev. Environ. Sci. Technol.* **2013**, 43 (9) 955– 1009 DOI: 10.1080/10643389.2011.627022

[Crossref], [CAS]

12. 12.

Beller, H. R.; Han, R.; Karaoz, U.; Lim, H.; Brodie, E. L. Genomic and Physiological Characterization of the Chromate-Reducing, Aquifer-Derived Firmicute Pelosinus sp. Strain HCF1 *Appl. Environ. Microbiol.* **2013**,79 (1) 63– 73 DOI: 10.1128/AEM.02496-12

[Crossref], [PubMed], [CAS]

13. 13.

Han, R.; Geller, J. T.; Yang, L.; Brodie, E. L.; Chakraborty, R.; Larsen, J. T.; Beller, H. R. Physiological and Transcriptional Studies of Cr(VI) Reduction under Aerobic and Denitrifying Conditions by an Aquifer-Derived Pseudomonad *Environ. Sci. Technol.* **2010**, 44 (19) 7491– 7497 DOI: 10.1021/es101152r

[ACS Full Text], [CAS]

14. 14.

Palmer, C. D.; Wittbrodt, P. R. Processes affecting the remediation of chromium-contaminated sites *Env. Heal. Perspect.* **1991**, 92, 25– 40 DOI: 10.1289/ehp.919225

[Crossref], [CAS]

15. 15.

Schroeder, D. C.; Lee, G. F. Potential transformations of chromium in natural waters *Water, Air, Soil Pollut.***1975**, 4 (3) 355– 365 DOI: 10.1007/BF00280721

[Crossref], [CAS]

16. 16.

Eary, L. E.; Rai, D. Kinetics of chromium(III) oxidation to chromium(VI) by reaction with manganese dioxide*Environ. Sci. Technol.* **1987**, 21 (12) 1187– 1193 DOI: 10.1021/es00165a005

[ACS Full Text]

17. 17.

Stewart, B. D.; Nico, P. S.; Fendorf, S. Stability of Uranium Incorporated into Fe (Hydr)oxides under Fluctuating Redox Conditions *Environ. Sci. Technol.* **2009**, 43 (13) 4922– 4927 DOI: 10.1021/es803317w

[ACS Full Text], [CAS]

18. 18.

Borch, T.; Kretzschmar, R.; Kappler, A.; Cappellen, P. Van; Ginder-Vogel, M.; Voegelin, A.; Campbell, K.Biogeochemical Redox Processes and their Impact on Contaminant Dynamics *Environ. Sci. Technol.* **2010**,44 (1) 15– 23 DOI: 10.1021/es9026248

[ACS Full Text], [CAS]

19. 19.

Fendorf, S. E.; Zasoski, R. J. Chromium(III) oxidation by.delta.-manganese oxide (MnO2). 1. Characterization *Environ. Sci. Technol.* **1992**, 26 (1) 79– 85 DOI: 10.1021/es00025a006

[ACS Full Text], [CAS]

20. 20.

Bartlett, R.; James, B. Behavior of Chromium in Soils: III. Oxidation *J. Environ. Qual.* **1979**, 8, 31– 35 DOI: 10.2134/jeq1979.00472425000800010008x

[Crossref], [CAS]

21. 21.

Fischel, J. S.; Fischel, M. H.; Sparks, D. L. Advances in Understanding Reactivity of Manganese Oxides with Arsenic and Chromium in Environmental Systems. In *Advances in the Environmental Biogeochemistry of Manganese Oxides*; ACS Symposium Series; American Chemical Society, **2015**; Vol. 1197, p 1.

[ACS Full Text]

22. 22.

Butler, E. C.; Chen, L.; Hansel, C. M.; Krumholz, L. R.; Elwood Madden, A. S.; Lan, Y. Biological versus mineralogical chromium reduction: potential for reoxidation by

manganese oxide *Environ. Sci. Process. Impacts* **2015**, 17 (11) 1930– 1940 DOI: 10.1039/C5EM00286A

[Crossref], [PubMed], [CAS]

23. 23.

Dai, R.; Liu, J.; Yu, C.; Sun, R.; Lan, Y.; Mao, J.-D. A comparative study of oxidation of Cr(III) in aqueous ions, complex ions and insoluble compounds by manganese-bearing mineral (birnessite) *Chemosphere***2009**, 76 (4) 536– 541 DOI: 10.1016/j.chemosphere.2009.03.009

[Crossref], [PubMed], [CAS]

24. 24.

Feng, X. H.; Zhai, L. M.; Tan, W. F.; Liu, F.; He, J. Z. Adsorption and redox reactions of heavy metals on synthesized Mn oxide minerals *Environ. Pollut.* **2007**, 147 (2) 366– 373 DOI: 10.1016/j.envpol.2006.05.028

[Crossref], [PubMed], [CAS]

25. 25.

Kim, J. G.; Dixon, J. B.; Chusuei, C. C.; Deng, Y. Oxidation of Chromium(III) to (VI) by Manganese Oxides*Soil Sci. Soc. Am. J.* **2002**, 66, 306– 315 DOI: 10.2136/sssaj2002.0306

[Crossref], [CAS]

26. 26.

Banerjee, D.; Nesbitt, H. W. Oxidation of aqueous Cr(III) at birnessite surfaces: constraints on reaction mechanism *Geochim. Cosmochim. Acta* **1999**, 63 (11–12) 1671– 1687 DOI: 10.1016/S0016-7037(99)00003-4

[Crossref], [CAS]

27. 27.

Rajapaksha, A. U.; Vithanage, M.; Ok, Y. S.; Oze, C. Cr(VI) Formation Related to Cr(III)-Muscovite and Birnessite Interactions in Ultramafic Environments *Environ. Sci. Technol.* **2013**, 47 (17) 9722– 9729 DOI: 10.1021/es4015025

[ACS Full Text], [CAS]

28. 28.

Fendorf, S. E.; Fendorf, M.; Sparks, D. L.; Gronsky, R. Inhibitory mechanisms of Cr(III) oxidation by δ-MnO2*J. Colloid Interface Sci.* **1992**, 153 (1) 37– 54 DOI: 10.1016/0021-9797(92)90296-X

[Crossref], [CAS]

29. 29.

Namgung, S.; Kwon, M. J.; Qafoku, N. P.; Lee, G. Cr(OH)3(s) Oxidation Induced by Surface Catalyzed Mn(II) Oxidation *Environ. Sci. Technol.* **2014**, 48 (18) 10760– 10768 DOI: 10.1021/es503018u

[ACS Full Text], [CAS]

30. 30.

Landrot, G.; Ginder-Vogel, M.; Sparks, D. L. Kinetics of Chromium(III) Oxidation by Manganese(IV) Oxides Using Quick Scanning X-ray Absorption Fine Structure Spectroscopy (Q-XAFS) *Environ. Sci. Technol.* **2010**,44 (1) 143– 149 DOI: 10.1021/es901759w

[ACS Full Text], [CAS]

31. 31.

Wu, Y.; Deng, B.; Xu, H.; Kornishi, H. Chromium(III) Oxidation Coupled with Microbially Mediated Mn(II) Oxidation *Geomicrobiol. J.* **2005**, 22 (3–4) 161– 170 DOI: 10.1080/01490450590945997

[Crossref], [CAS]

32. 32.

Tang, Y.; Webb, S. M.; Estes, E. R.; Hansel, C. M. Chromium(iii) oxidation by biogenic manganese oxides with varying structural ripening *Environ. Sci. Process. Impacts* **2014**, 16 (9) 2127– 2136 DOI: 10.1039/C4EM00077C

[Crossref], [PubMed], [CAS]

33. 33.

Murray, K. J.; Tebo, B. M. Cr(III) Is Indirectly Oxidized by the Mn(II)-Oxidizing Bacterium Bacillus sp. Strain SG-1 *Environ. Sci. Technol.* **2007**, 41 (2) 528– 533 DOI: 10.1021/es0615167

[ACS Full Text], [CAS]

34. 34.

Sass, B. M.; Rai, D. Solubility of amorphous chromium(III)-iron(III) hydroxide solid solutions *Inorg. Chem.***1987**, 26 (14) 2228– 2232 DOI: 10.1021/ic00261a013

[ACS Full Text], [CAS]

35. 35.

Rai, D.; Sass, B. M.; Moore, D. A. Chromium(III) hydrolysis constants and solubility of chromium(III) hydroxide *Inorg. Chem.* **1987**, 26 (3) 345– 349 DOI: 10.1021/ic00250a002

[ACS Full Text], [CAS]

36. 36.

James, B. R.; Bartlett, R. J. Behavior of Chromium in Soils. VI. Interactions Between Oxidation-Reduction and Organic Complexation *J. Environ. Qual.* **1983**, 12, 173– 176 DOI: 10.2134/jeq1983.00472425001200020004x

[Crossref], [CAS]

37. 37.

Fendorf, S. E. Surface reactions of chromium in soils and waters *Geoderma* **1995**, 67 (1) 55– 71 DOI: 10.1016/0016-7061(94)00062-F

[Crossref], [CAS]

38. 38.

Charlet, L.; Manceau, A. A. X-ray absorption spectroscopic study of the sorption of Cr(III) at the oxide-water interface: II. Adsorption, coprecipitation, and surface precipitation on hydrous ferric oxide *J. Colloid Interface Sci.* **1992**, 148 (2) 443– 458 DOI: 10.1016/0021-9797(92)90182-L

[Crossref], [CAS]

39. 39.

Fendorf, S. E.; Zasoski, R. J.; Burau, R. G. Competing Metal Ion Influences on Chromium(III) Oxidation by Birnessite *Soil Sci. Soc. Am. J.* **1993**, 57, 1508– 1515 DOI: 10.2136/sssaj1993.03615995005700060019x

[Crossref], [CAS]

40. 40.

Feng, X. H.; Zhai, L. M.; Tan, W. F.; Zhao, W.; Liu, F.; He, J. Z. The controlling effect of pH on oxidation of Cr(III) by manganese oxide minerals *J. Colloid Interface Sci.* **2006**, 298 (1) 258– 266 DOI: 10.1016/j.jcis.2005.12.012

[Crossref], [PubMed], [CAS]

41. 41.

Tokunaga, T. K.; Wan, J.; Lanzirotti, A.; Sutton, S. R.; Newville, M.; Rao, W. Long-Term Stability of Organic Carbon-Stimulated Chromate Reduction in Contaminated Soils and Its Relation to Manganese Redox Status *Environ. Sci. Technol.* **2007**, 41 (12) 4326– 4331 DOI: 10.1021/es062874c

[ACS Full Text], [CAS]

42. 42.

Beller, H. R.; Yang, L.; Varadharajan, C.; Han, R.; Lim, H. C.; Karaoz, U.; Molins, S.; Marcus, M. A.;Brodie, E. L.; Steefel, C. I.Divergent Aquifer Biogeochemical Systems Converge on Similar and Unexpected Cr(VI) Reduction Products *Environ. Sci. Technol.* **2014**, 48 (18) 10699– 10706 DOI: 10.1021/es5016982

[ACS Full Text], [CAS]

43. 43.

Varadharajan, C.; Han, R.; Beller, H. R.; Yang, L.; Marcus, M. A.; Michel, M.; Nico, P. S. Characterization of Chromium Bioremediation Products in Flow-Through Column Sediments Using Micro–X-ray Fluorescence and X-ray Absorption Spectroscopy *J. Environ. Qual.* **2015**, 44, 729– 738 DOI: 10.2134/jeq2014.08.0329

[Crossref], [PubMed], [CAS]

44. 44.

Dresel, P. E.; Ainsworth, C. C.; Qafoku, N. P.; Liu, C.; McKinley, J. P.; Itlton, E. S.; Fruchter, J. S.;Phillips, J. L. Geochemical Characterization of Chromate Contamination in the 100 Area Vadose Zone at the Hanford Site; Richland, WA, **2008**.

[Crossref]

45. 45.

Lovley, D. R.; Phillips, E. J. P. Rapid Assay for Microbially Reducible Ferric Iron in Aquatic Sediments *Appl. Environ. Microbiol.* **1987**, 53 (7) 1536– 1540

[PubMed], [CAS]

46. 46.

Nico, P. S.; Zasoski, R. J. Importance of Mn(III) Availability on the Rate of Cr(III) Oxidation on δ-MnO2*Environ. Sci. Technol.* **2000**, 34 (16) 3363– 3367 DOI: 10.1021/es991462j

[ACS Full Text], [CAS]

47. 47.

Torn, M. S.; Davis, S.; Bird, J. A.; Shaw, M. R.; Conrad, M. E. Automated analysis of 13C/12C ratios in CO2 and dissolved inorganic carbon for ecological and environmental applications *Rapid Commun. Mass Spectrom.* **2003**, 17 (23) 2675– 2682 DOI: 10.1002/rcm.1246

[Crossref], [PubMed], [CAS]

48. 48.

Hornung, R. W.; Reed, L. D. Estimation of Average Concentration in the Presence of Nondetectable Values*Appl. Occup. Environ. Hyg.* **1990**, 5 (1) 46– 51 DOI: 10.1080/1047322X.1990.10389587

[Crossref], [CAS]

49. 49.

Hausladen, D. M.; Fendorf, S. Hexavalent Chromium Generation within Naturally Structured Soils and Sediments *Environ. Sci. Technol.* **2017**, 51, 2058 DOI: 10.1021/acs.est.6b04039

[ACS Full Text], [CAS]

50. 50.

Wu, Y.; Deng, B. Inhibition of FeS on Chromium(III) Oxidation by Biogenic Manganese Oxides *Environ. Eng. Sci.* **2006**, 23 (3) 552– 560 DOI: 10.1089/ees.2006.23.552

[Crossref], [CAS]

51. 51.

Williams, M. D.; Rockhold, M. L.; Thorne, P. D.; Chen, Y. Three-Dimensional Groundwater Models of the 300 Area at the Hanford Site, Washington State - PNNL-17708; United States, **2008**.

[Crossref]